Characterization of Dihydrogen–Bonded D–H$\cdots$H–A Complexes on the Basis of Spectroscopic Parameters

IUPAC Workshop “Hydrogen Bonding and other Molecular Interactions”

5–9.09.2005, Pisa

Joanna Sadlej

Department of Chemistry, University of Warsaw, Pasteura 1, 02-093 Warsaw, Poland

Motto

A few observation and much reasoning
lead to error
many observations and a little reasoning
to truth.

Alexis Carrel

Overview

- Motivations
- Spectroscopic evidence for the existence of H-bond
- The indirect nuclear spin–spin coupling constants transmitted through H-bond.
- The calculations of the SSCC
- Dihydrogen bonds (DHB) - structures and energetics
- Spectroscopic characterization of DHB complexes
- What is the long–range asymptotic behaviour of spin–spin couplings?
- Conclusions about DHB and ^{h}J as a parameter which characterize the H bonds

Motivation

- Numerous spectroscopic techniques provided **indirect** evidence for existence of H–bond: the changes of parameters of **monomers induced** by the intermolecular interactions.
- The indirect spin–spin coupling constants transmitted through H–bond are used as the **direct** evidence of hydrogen bonds.
- Dihydrogen bonds (DHB), where D–H acts as a proton donor and A–H as a proton acceptor, have been subject of many investigations.
- The question is: is there a fundamental difference between DHB, conventional H-bonds and other van der Waals systems?

Spectroscopic evidence for the existence of H–bond

Usually, the existence of H–bond is inferred *a posteriori* from spatial proximity and relative orientation of the H–bond donor, hydrogen and the H–bond acceptor.

Very few experimental parameters exist, which can provide an evidence of individual hydrogen bonds, and thus identify all atoms involved in H–bond, X–H$\cdots$Y.

Spectroscopic evidence for the existence of H–bond

A number of spectroscopic observables provides an indirect evidence for individual, conventional H–bonds:

- the red–shift of the X–H stretch vibration, which varies between several tens or hundreds of wavenumbers, since the formation of a H–bond in a X–H $\cdots$ Y system is accompanied by weakening of the X–H covalent bond,
- the increase of the IR intensity of the X–H stretch,
- the 'downfield' shift of the ^{1}H NMR caused by proton deshielding (reduced σ_{iso}),
- the reduced hydrogen exchange rates with the solvent,
- the primary isotope shifts for substitution of the hydrogen bonded proton by ^{2}H in NMR and vibrational spectra.

Spectroscopic evidence for the existence of H–bond

All methods mentioned above rely on detection the H-bond through changes in **some properties of monomers**.

New spectroscopic parameters — intermolecular indirect spin–spin coupling constants provide an unique **direct** experimental evidence for H–bond formation.

The interest in the intermolecular indirect spin-spin coupling constants (ISSCC) has grown in 1998, when these couplings were measured between nuclei belonging to complementary pairs of nucleic bases in RNA and DNA.

A. J. Dingley, S. Grzesiek, Direct observation of hydrogen bonds in nuclear acid base pairs by internucleotide $^{2}\mathrm{J}_{NN}$ coupligs, J. Amer. Chem. Soc., 120, (1998) 8293.

The intermolecular indirect spin-spin coupling constants

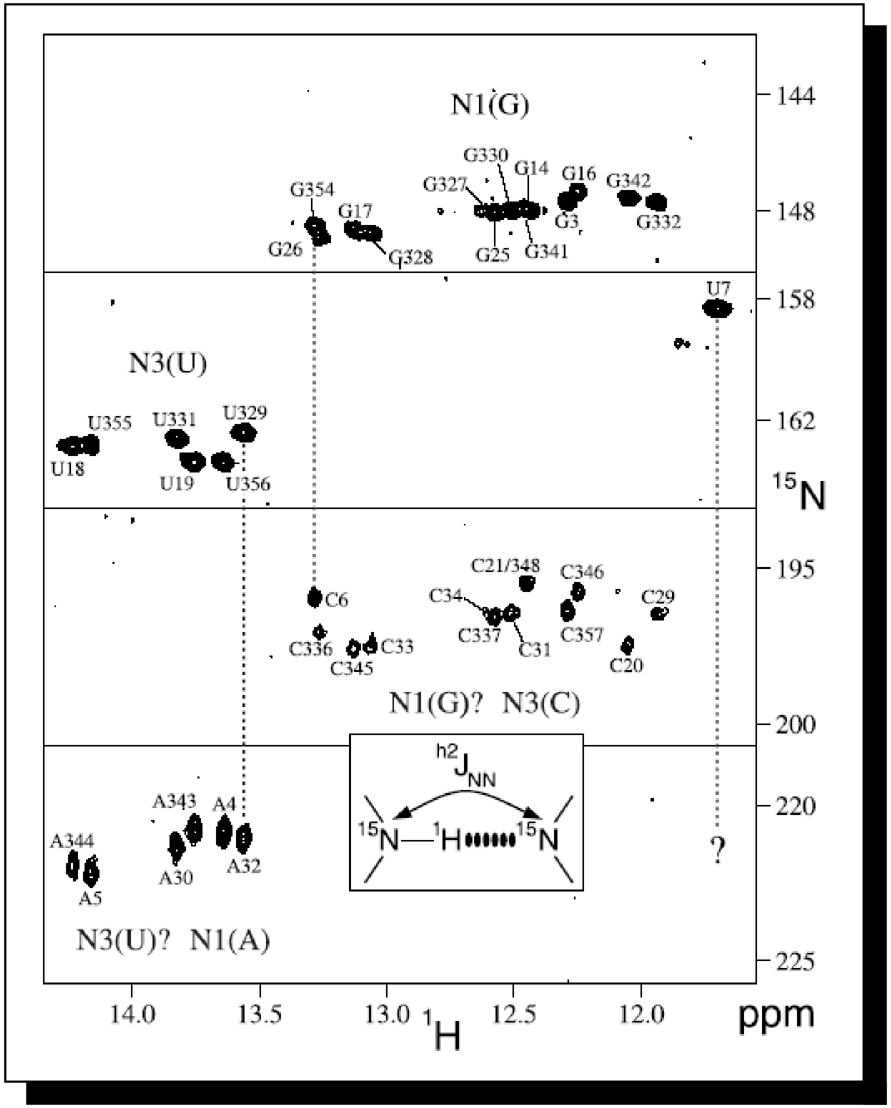

The intermolecular indirect spin-spin coupling constants

— the surprisingly large values of the couplings ${}^{2h}\mathrm{J}_{NN}$, ${}^{15}\mathrm{N}\cdots{}^{15}\mathrm{N}$ hydrogen–bond transmitted couplings fall within 6–7 Hz range

— ...“the J couplings unambiguously establish the partial covalent character of such interactions” CEN, S. Borman, 77, 36 (1999).
NMR coupling constants transmitted through hydrogen bond is a fingerprint for specifying H–bond type.

- **[1] J. E. Del Bene, S. A. Perera, R. J. Bartlett, I. Alkorta, J. Elguero, O. Mo, M. Yanez, J. Phys. Chem., A, 2002, 106, 9331-9337; and many others papers**
- **[2] M. Pecul, J. Sadlej, Computation Chemistry, Review of Current Trends, vol. 8, ed. J. Leszczynski, World Scientific, N. Y. 2003**

Definitions of NMR parameters

Together, $\boldsymbol{\sigma}_P$ and $\mathbf{K}_{PQ}$ determine the spin Hamiltonian of high-resolution NMR: $\mathbf{M}$-nuclear moment, $\mathbf{B}$-magnetic induction

$$\mathcal{H}_{\mathrm{NMR}} = -\mathbf{B}^{\mathrm{T}} \sum_{P} (\mathbf{1} - \boldsymbol{\sigma}_P)\mathbf{M}_P + \sum_{P>Q} \mathbf{M}_P^{\mathrm{T}} \mathbf{K}_{PQ} \mathbf{M}_Q$$

- experimentalists determine $\boldsymbol{\sigma}_P$ and $\mathbf{K}_{PQ}$ from observed spectra
- we can determine these parameters from the molecular electronic structure as energy derivatives

$$\mathbf{E}_{KL}^{(02)} = \left.\frac{d^2 E\,(\mathbf{B}, \mathbf{M})}{d\mathbf{M}_K\, d\mathbf{M}_L}\right|_{\mathbf{B}=\mathbf{0},\mathbf{M}=\mathbf{0}} \quad (1)$$

$$\mathbf{E}_{KL}^{(20)} = \left.\frac{d^2 E\,(\mathbf{B}, \mathbf{M})}{d\mathbf{B}\, d\mathbf{B}}\right|_{\mathbf{B}=\mathbf{0},\mathbf{M}=\mathbf{0}} \quad (2)$$

(3)

Ramsey's perturbation theory

The expression for the indirect spin–spin coupling tensors $\mathbf{K}_{PQ}$ (Ramsey, 1953):

$$\begin{aligned}
\mathbf{K}_{PQ} &= \left\langle 0 \left| \mathbf{h}_{PQ}^{\mathrm{DSO}} \right| 0 \right\rangle \quad \text{DSO} \\
&+ 2 \sum_{n_{\mathrm{S}} \neq 0} \frac{\left\langle 0 \left| \mathbf{h}_{P}^{\mathrm{PSO}} \right| n_{\mathrm{S}} \right\rangle \left\langle n_{\mathrm{S}} \left| (\mathbf{h}_{Q}^{\mathrm{PSO}})^{\mathrm{T}} \right| 0 \right\rangle}{E_{n_{\mathrm{S}}} - E_0} \quad \text{PSO} \\
&+ 2 \sum_{n_{\mathrm{T}}} \frac{\left\langle 0 \left| \mathbf{h}_{P}^{\mathrm{FC}} + \mathbf{h}_{P}^{\mathrm{SD}} \right| n_{\mathrm{T}} \right\rangle \left\langle n_{\mathrm{T}} \left| (\mathbf{h}_{Q}^{\mathrm{FC}})^{\mathrm{T}} + (\mathbf{h}_{Q}^{\mathrm{SD}})^{\mathrm{T}} \right| 0 \right\rangle}{E_{n_{\mathrm{T}}} - E_0} \text{FC, SD}
\end{aligned}$$

In 1950, Ramsey derived an expression for nuclear shieldings $\boldsymbol{\sigma}_P$, describing the interaction of the nuclei with an external magnetic field in the presence of electrons.In practice, spin–spin coupling constants are not calculated from Ramsey's expression, which involves a full summation over all singlet and triplet excited states

The contributions to spin–spin coupling constants

- The isotropic indirect spin–spin coupling constants can be uniquely decomposed as:

$$\mathbf{K}_{PQ} = \mathbf{K}_{PQ}^{\mathrm{DSO}} + \mathbf{K}_{PQ}^{\mathrm{PSO}} + \mathbf{K}_{PQ}^{\mathrm{FC}} + \mathbf{K}_{PQ}^{\mathrm{SD}}$$

- The spin–spin coupling constants are often dominated by the FC term.
- Since the FC term is relatively easy to calculate, it is tempting to ignore the other terms.
- However, none of the contributions can be *a priori* neglected

The contributions to spin–spin coupling constants

In experiment, the observed quantities are indirect spin–spin coupling tensors $\mathbf{J}_{PQ}$, which are related to the reduced tensors as

$$\mathbf{J}_{PQ} = \frac{1}{h}\mu_{\mathrm{N}} g_P \mu_{\mathrm{N}} g_Q \mathbf{K}_{PQ}$$

The reduced coupling tensors $\mathbf{K}_{PQ}$ are independent of the nuclear g factors.

Apart from the shielding constants, the SSCC represent the most important source of structural information of NMR. First, the magnitude of the SSCC depends on the electron distribution between the coupled nuclei; second, since SSCC are highly sensitive to the molecular geometry, they are extensively used in conformational studies.

Calculations of indirect spin–spin couplings - theory

- The calculation of spin–spin coupling constants is a challenging task:
  - triplet as well as singlet perturbations are involved
  - because of triplet-instability problems, the RHF model is unsuitable for spin–spin calculations
  - the dominant FC contribution requires an accurate description of the electron density at the nuclei (large decontracted s sets)
- We must solve a large number of response equations:
  - 3 singlet equations and 7 triplet equations for each nucleus → for large molecules we need to select nuclei of interest
  - (for shielding constants, only 3 equations are required)

Calculations of indirect spin–spin couplings - theory

- Spin–spin couplings are very sensitive to the molecular geometry:
  - equilibrium structures must be chosen carefully
  - large vibrational corrections (often 5%–10%)
- However, unlike in shielding calculations, there is no need for London orbitals since no external magnetic field is involved.
- For heavy elements, a relativistic treatment may be necessary

Correlated methods for spin–spin coupling calculations

- Hartree–Fock theory cannot be used → to obtain reliable results, we need correlated methods.
- Traditional wave-function methods:
  - SOPPA, MCSCF, CCSD, EOM-CCSD, CC3 and CCSDT
  - These methods are (at least for now) restricted to small systems.
  - Typical errors: a few Hz, but often 10%–20% for small couplings

Although the SSCC of small molecules can be calculated by methods high-level CC theory, the only methods currently capable of routinely treating systems containing more than ten to twenty atoms are those provided by DFT.

Correlated methods for spin–spin coupling calculations

DFT methods:

- errors are somewhat larger and less predictable than for the most accurate wave-function methods
- much less susceptible to triplet instabilities than Hartree–Fock theory; HF model is unreliable, often providing results that bear little resemblance to the true CC.
- DFT calculations are less expensive and applicable to large systems
- some problem areas persist with DFT, particular for the spin-spin couplings to electron-rich atoms such as the fluorine.

Programs

DALTON, an *ab initio* electronic structure program, T. Helgaker (Oslo) version, http://www.kjemi.uio.no/software/dalton/dalton.html.

T. Helgaker, H. J. A. Jensen, P. Jørgensen, J. Olsen, K. Ruud, H. Ågren, A. A. Auer, K. L. Bak, V. Bakken, O. Christiansen, S. Coriani, P. Dahle, E. K. Dalskov, T. Enevoldsen, B. Fernandez, C. Hättig, K. Hald, A. Halkier, H. Heiberg, H. Hettema, D. Jonsson, S. Kirpekar, R. Kobayashi, H. Koch, K. V. Mikkelsen, P. Norman, M. J. Packer, T. B. Pedersen, T. A. Ruden, A. Sanchez, T. Saue, S. P. A. Sauer, B. Schimmelpfenning, K. O. Sylvester-Hvid, P. R. Taylor, and O. Vahtras.

ACES II program package, J. Gauss (Mainz) version,

J. F. Stanton, J. Gauss, J. D. Watts, W. J. Lauderdale, and R. J. Bartlett. Int. J. Quantum Chem.:Quantum Chem. Symp., 26:879, 1992.

The intermolecular indirect spin-spin coupling constants

The spin–spin coupling constants for the hydrogen–bonded formamid–formamid (*Fa–Fa*) and formamid–formamidine (*Fa–Fi*) complexes (M. Pecul, J. Leszczynski and J. Sadlej, J. Phys. Chem **A**, 2000, **104**, 8105)

Fa–Fa is a model of hydrogen bonding in peptides, *Fa–Fi* serves as a model of interaction between the complementary pairs of nucleic basis.

The intermolecular indirect spin-spin coupling constants

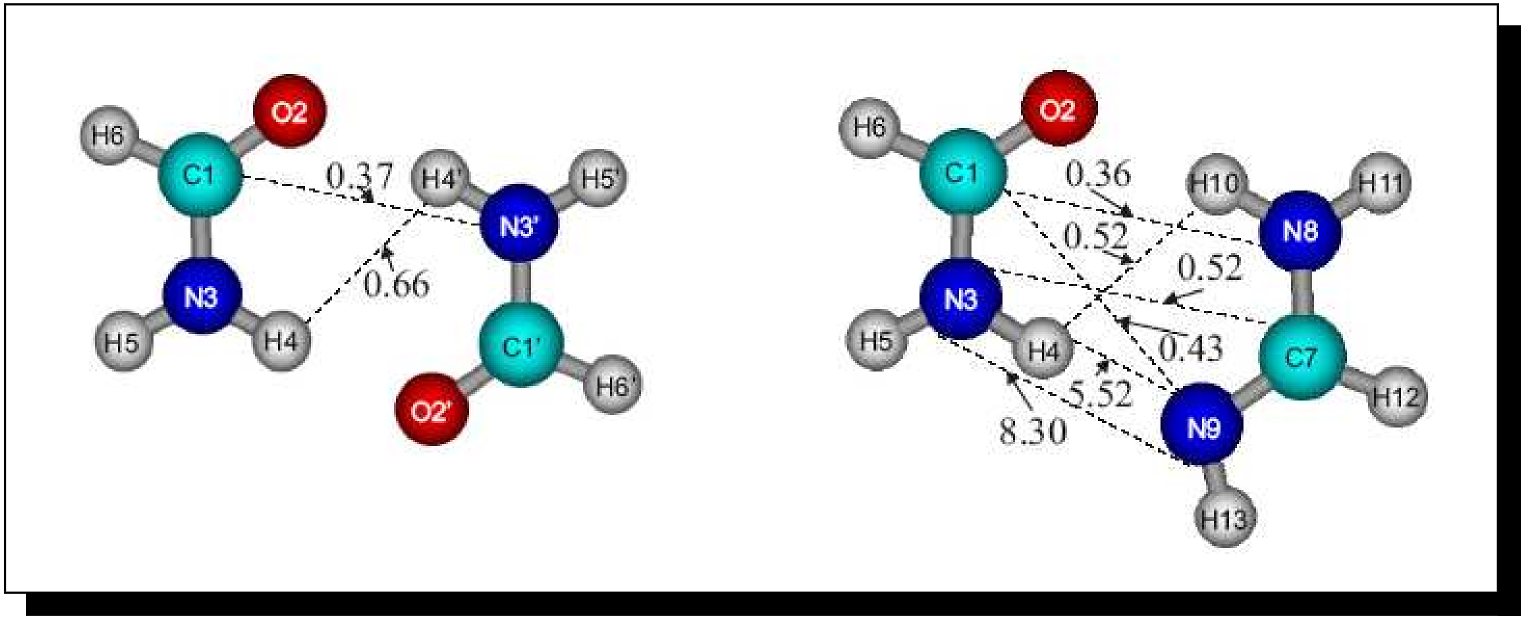

The spin–spin coupling constants were calculated using the linear response MC SCF method with aug-cc-pVDZsu1 basis set.

The intermolecular indirect spin-spin coupling constants

- The calculated ^{1h}J$_{NH}$ $=$5.5 Hz, ^{2h}J$_{NN}$ $=$8.3 Hz are in agreement with experimental for DNA (6.7 Hz for U–A, 1.3–3.6 Hz for DNA).
- The discussed hydrogen–bond–transmitted coupling constants are dominated by Fermi–contact term.
- The SSCC transmitted through H-bond provides a fingerprint for hydrogen bond type.
- The intermolecular hydrogen–bond–transmitted coupling constants between protons engaged in the H–bonds have not been detected experimentally — our results indicate that these couplings should have measured values.

Dihydrogen bonds (DHB)

In the middle of the 1990s a new kind of molecular interactions was described.

$$\mathrm{D}—\mathrm{H}^{\delta+}\cdots\mathrm{H}^{\delta-}—\mathrm{A}$$

This type of interaction was termed a DHB because the link between the molecules within the complex is realized through the H$\cdots$H contact.

D–H is a typical proton–donating molecule (such as O–H, N–H), while A–H acts as a proton acceptor — typical element A is the transition metal or boron (A=Ir, Mo, Re, Li, Na, K, B).

Dihydrogen bonds (DHB)

From X–ray and neutron diffraction studies it is known that the H$\cdots$H distances in DHB are usually shorter than 2 Å which is significantly smaller than the sum of two van der Waals radii of the hydrogen atoms.

Species with DHBs may sometimes be transformed into covalently bound materials, thereby opening new opportunities in material sciences.

There is number of papers concerning DHB systems:

“Dihydrogen bonding: structures, energetics and dynamics” R. Custelcean and J. E. Jackson, Chem. Rev., 2001, 101, 1963

Dihydrogen bonds (DHB)

We address the following questions:

1. Is there a fundamental difference between DHBs, conventional H–bonds and van der Waals complexes? Is DHB a different face of hydrogen bond?

2. Do DHBs share the properties of conventional H–bonds?

3. How they differ from weak van der Waals complexes?

To explore these issues we have examined the spectroscopic properties of the model DHB complexes, including their interaction energy and its decomposition into physically meaningful terms.

The model dihydrogen–bonded complexes

We investigated complexes of LiH or BeH_2 molecules as proton acceptors and different molecules as proton donors.

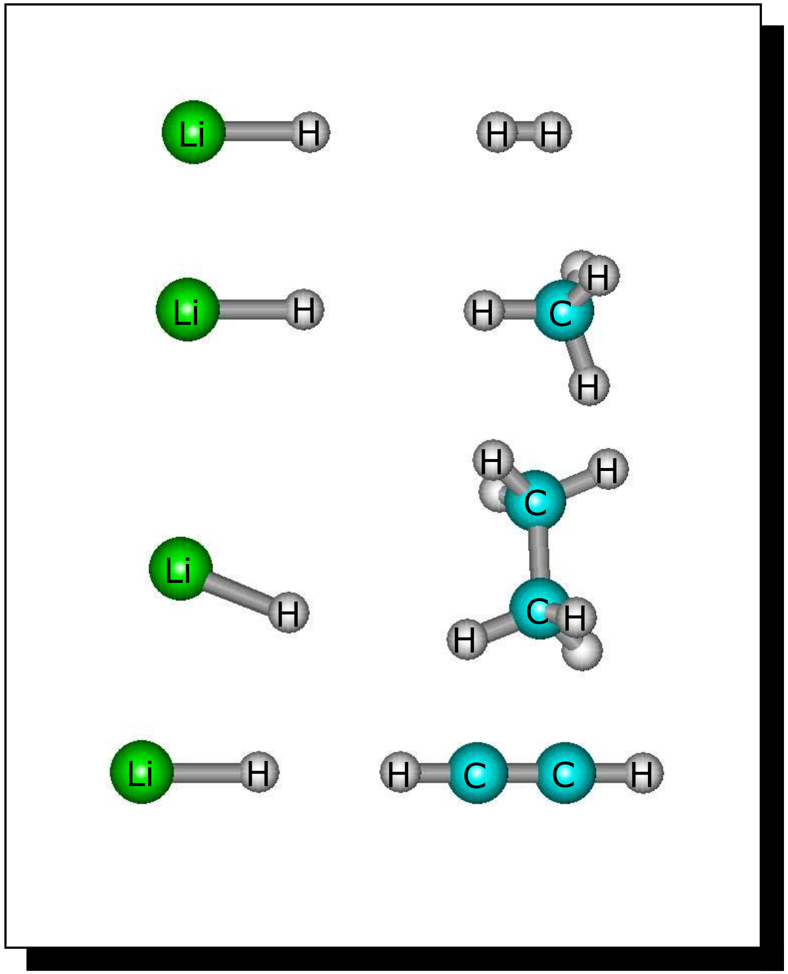

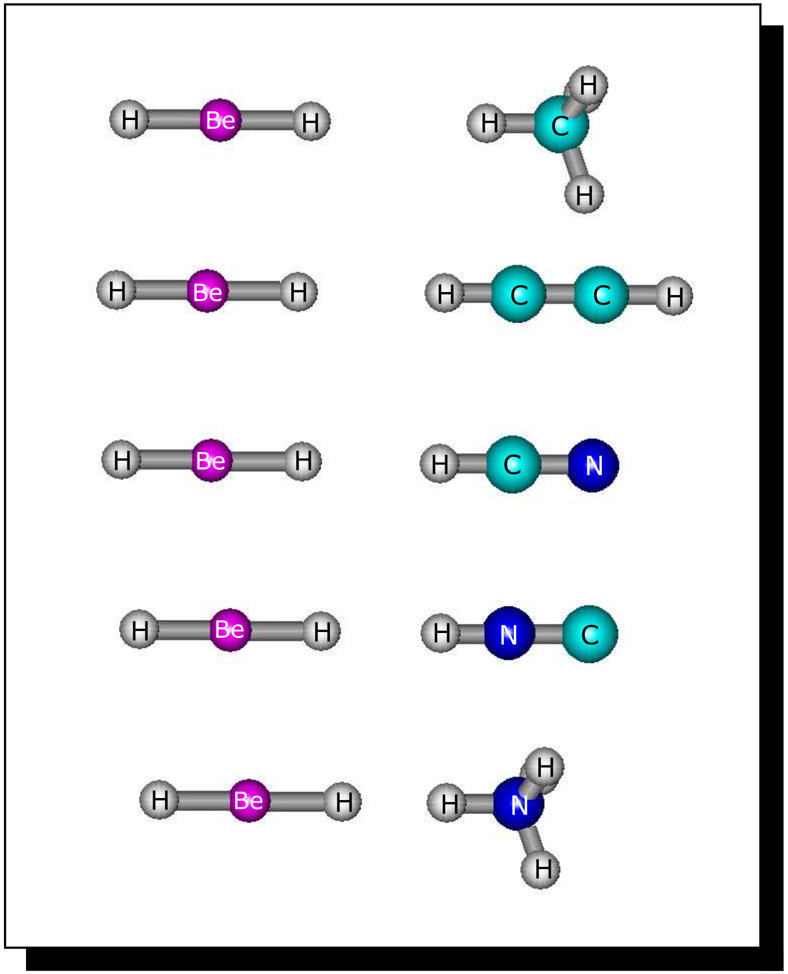

The geometry of the complexes

The $H\cdots H$ intermolecular distance decreases as the interaction energy increases:

- the longest $H\cdots H$ intermolecular distances are present in dimers which can be classified as the weak van der Waals complexes ($LiH\cdots CH_4$, $BeH_2\cdots C_2H_2$,)
- in the dihydrogen–bonded complexes, comparable with the conventional H–bonds ($LiH\cdots C_2H_2$, $BeH_2\cdots HCN$) the $H\cdots H$ intermolecular distance is ca. 2 Å,
- the shortest $H\cdots H$ distance ca. 1.55 Å is observed in the very strong complex of $BeH_2\cdots NH_4^+$.

The geometry of the complexes

complex	method	r(H$\cdots$H)(Å)	r(Li-H)(Å)	r(H-X)(Å)
LiH$\cdots$CH$_4$	MP2	2.5093	1.6052 (+0.0003)	1.0872 (+0.0010)
	MP4	2.4936	1.6088 (+0.0003)	1.0905 (+0.0008)
	CCSD	2.5794	1.6104 (-0.0001)	1.0888 (+0.0003)
	B3LYP	2.6287	1.5894 (-0.0005)	1.0886 (+0.0003)
LiH$\cdots$C$_2$H$_2$	MP2	1.9721	1.6017 (-0.0032)	1.0733 (+0.0116)
	MP4	1.9758	1.6047 (-0.0037)	1.0752 (+0.0113)
	CCSD	2.0370	1.6060 (-0.0045)	1.0715 (+0.0094)
	B3LYP	2.0040	1.5848 (-0.0051)	1.0734 (+0.0118)

The comparison of the methods: all the calculations were performed with the aug-cc-pVTZ basis set

The geometry of the complexes

complex	r(H$\cdots$H)(Å)	r(Be—H)(Å)	r(H—X)(Å)
$BeH_2\cdots H_2$	2.6716	1.3293 (-0.0001)	0.7381 (+0.0006)
$BeH_2\cdots CH_4$	2.5903	1.3294 (+0.0001)	1.0863 (+0.0001)
$BeH_2\cdots C_2H_2$	2.1740	1.3294 (+0.0001)	1.0637 (+0.0020)
$BeH_2\cdots HCN$	2.0311	1.3311 (+0.0017)	1.0677 (+0.0031)
$BeH_2\cdots HNC$	1.7704	1.3308 (+0.0014)	1.0051 (+0.0075)
$BeH_2\cdots NH_4^+$	1.5592	1.3523 (+0.0229)	1.0415 (+0.0196)

The calculations were performed at MP2/aug-cc-pVTZ level

if the donors are listed in order of increasing proton-donating ability to LiH or to BeH_2, then the H$\cdots$H distance decreases from 2.6 Å in $BeH_2\cdots CH_4$ to 1.8 Å in $BeH_2\cdots HNC$.

The interaction energy

parameter	complex	MP2	MP4	CCSD	B3LYP
$D_e(kJ/mol)$	$LiH\cdots CH_4$	-3.20	-3.48	-2.84	-1.48
	$BeH_2\cdots C_2H_2$	-4.69			
	$BeH_2\cdots HCN$	-8.39			
	$LiH\cdots C_2H_2$	-17.78	-17.82	-16.04	-15.27
	$BeH_2\cdots NH_4^+$	-41.78			
$D_0(kJ/mol)$	$LiH\cdots CH_4$	-0.83	-1.25	-0.58	0.81
	$BeH_2\cdots C_2H_2$	-1.58			
	$BeH_2\cdots HCN$	-4.78			
	$LiH\cdots C_2H_2$	-13.17	-13.16	-11.5	-11.03
	$BeH_2\cdots NH_4^+$	-37.03			

All the calculations were performed with the aug-cc-pVTZ basis set

The energetics of the complexes

The dissociation energy D_0 increases in the sequence:

$BeH_2 \cdots H_2 < BeH_2 \cdots CH_4 < LiH \cdots H_2 < LiH \cdots C_2H_6 <$
$BeH_2 \cdots C_2H_2 < BeH_2 \cdots HCN < BeH_2 \cdots HNC < LiH \cdots C_2H_2$
$< BeH_2 \cdots NH_4^+$

The interaction energy

The complexes can be divided into three groups:

- weak van der Waals complexes (LiH$\cdots$CH$_4$, BeH$_2\cdots$C$_2$H$_2$), the binding energies ca 1kJ/mol,
- dihydrogen–bonded complexes, comparable with the conventional H–bonds (LiH$\cdots$C$_2$H$_2$, BeH$_2\cdots$HCN), D$_e$ ca 3-30 kJ/mol,
- very strong complex of BeH$_2\cdots$NH$_4^+$, which can be classified as very strong hydrogen bond; D$_e$ ca 30-50 kJ/mol.
- the binding energies of the complexes with C-H$\cdots$H-Li / Be dihydrogen bond vary quadratically with the H$\cdots$ distance.

The interaction energy

- The differences between MP2 (MP4), CCSD and B3LYP are substantial.
- DFT performs well for the strong LiH$\cdots$$C_2H_2$ complex.
- DFT is incapable of a correct description of dispersion, which plays crucial role in stabilizing weak van der Waals complexes.

SAPT calculations

The intermolecular interaction energy $E_{\text{int}}^{\text{SAPT}}$ was represented by the sum of the first– and second–order polarization and exchange contributions,

$$E_{\text{int}}^{\text{SAPT}} = E_{\text{int}}^{\text{HF}} + E_{\text{int}}^{\text{corr}} =$$

$$E_{\text{elst}}^{(10)} + E_{\text{exch}}^{(10)} + E_{\text{ind,r}}^{(20)} + E_{\text{exch}-\text{ind}}^{(20)} + E_{\text{disp}}^{(20)} + E_{\text{exch}-\text{disp}}^{(20)} + \ldots$$

were: $E_{\text{elst}}^{(10)}$ is the classical (Coulomb) electrostatic energy,
$E_{\text{exch}}^{(10)}$ is the exchange term results from the antisymmetrization of the wave function,
$E_{\text{ind,r}}^{(20)}$ and $E_{\text{disp}}^{(20)}$ denote the non–expanded induction (with response) and dispersion energies, and $E_{\text{exch}-\text{ind}}^{(20)}$, and $E_{\text{exch}-\text{disp}}^{(20)}$ are the second–order exchange–induction (with response), and exchange–dispersion energies.

The contributions appearing on the right–hand side were evaluated using the many–body techniques; B. Jeziorski, R. Moszynski, K. Szalewicz, Chem. Rev., **1994**, 94, 5498.

The decomposition of the total interaction energy

Term (kJ/mol)	**$(H_2O)_2$**	**$LiH\cdot CH_4$**	**$LiH\cdot C_2H_2$**	**$BeH_2\cdot CH_4$**	**$BeH_2\cdot HCN$**	**$BeH_2\cdot NH_4^+$**
$\mathbf{E}^{(10)}_{elst}$	-35.10	-4.08	-28.59	-1.14	-11.65	-36.79
$\mathbf{E}^{(10)}_{exch}$	29.62	6.83	26.01	2.29	10.22	38.62
$\mathbf{E}^{(20)}_{ind,r}$	-12.69	-3.11	-13.43	-0.31	-4.72	-41.48
$\mathbf{E}^{(20)}_{disp}$	-10.74	-4.34	-10.07	-2.13	-4.80	-10.54
$\mathbf{E}^{(20)}_{exch-ind,r}$	6.98	1.39	8.47	0.15	2.24	16.75
$\mathbf{E}^{(20)}_{exch-disp}$	1.96	0.73	2.21	0.20	0.61	1.66
Sum	**-19.99**	**-2.58**	**-15.39**	**-0.93**	**-8.10**	**-31.78**
$E^{(10)}_{elst}+E^{(10)}_{exch}$	-5.49	2.75	-2.58	1.15	-1.43	1.83

All the calculations were performed with the aug-cc-pVTZ basis set

The decomposition of the total interaction energy

The classification of the complexes into three groups is still valid:

- in weak van der Waals complexes (LiH$\cdots$CH$_4$, BeH$_2\cdots$C$_2$H$_2$) the first–order exchange term outweights the electrostatic one but the addition of the dispersion term makes the interaction energy negative
- in the dihydrogen–bonded complexes, comparable with the conventional H–bonds (LiH$\cdots$C$_2$H$_2$, BeH$_2\cdots$HCN) the main binding energy comes from the electrostatic energy followed by the induction and dispersion energy
- in the very strong complex of BeH$_2\cdots$NH$_4^+$ the first–order exchange term outweights the electrostatic one, but the attractive induction term is the largest

The vibrational harmonic frequencies

- The complexation causes the blue–shift of H acceptor, ν(Li–H) or ν(Be–H).
- The stretching frequencies ν_s and ν_{as} in proton donors molecules are red–shifted and the intensity of the C-H stretch band is greater in the complex relative to the monomer. That is, the same IR spectroscopic signature of the shift to lower frequency and increase in the intensity of the (X-H) stretch band upon formation of a traditional hydrogen bond is found. Moreover, the frequency shift increases with increases C-H distance and increasing binding energy of the complex.
- These shifts in frequencies for proton donor and proton acceptor molecules correlate to some extent with the interaction energy.

The vibrational harmonic frequencies

$LiH\cdots CH_4$	$\Delta\nu$(cm^{-1})			**$LiH\cdots C_2H_2$**	$\Delta\nu$(cm^{-1})		
	Li–H	donor			Li–H	donor	
MP2	8	ν_s(CH)	-12	MP2	49	ν(C$\equiv$C)	-23
		ν_{as}(CH)	-12			ν_{as}(CH)	-129
		ν_{as}(CH)	-9			ν_s(CH)	-40
MP4	9	ν_s(CH)	-12	MP4	53	ν(C$\equiv$C)	-24
		ν_{as}(CH)	-13			ν_{as}(CH)	-120
		ν_{as}(CH)	-6			ν_s(CH)	-40
CCSD	9	ν_s(CH)	-10	CCSD	53	ν(CC)	-19
		ν_{as}(CH)	-13			ν_{as}(CH)	-92
		ν_{as}(CH)	0			ν_s(CH)	-38
B3LYP	9	v$_s$(CH)	-10	B3LYP	48	ν(CC)	-25
		ν_{as}(CH)	-12			ν_{as}(CH)	-137
		ν_{as}(CH)	-3			ν_s(CH)	-37

All the calculations were performed with the aug-cc-pVTZ basis set

The vibrational harmonic frequencies

complex	$\Delta\nu$(Be–H)(cm^{-1})		$\Delta\nu$(donor)(cm^{-1})	
$BeH_2 \cdots CH_4$	ν_s(Be—H)	3	ν_s(C—H)	-2
	ν_{as}(Be—H)	5	ν_{as}(C—H)	-3
			ν_{as}(C—H)	0
$BeH_2 \cdots C_2H_2$	ν_s(Be—H)	13	ν(C—C)	-5
	ν_{as}(Be—H)	12	ν_{as}(C—H)	-13
			ν_s(C—H)	-14
$BeH_2 \cdots NH_4^+$	ν_s(Be—H)	-4	ν_s(N—H)	-274
	ν_{as}(Be—H)	27	ν_{as}(N—H)	-81
			ν_{as}(N—H)	19

The calculations were performed MP2/aug-cc-pVTZ level

The NMR shielding constants

complex	$\Delta\sigma$(Li–**H**)	$\Delta\sigma$(**H**–X)	$\Delta\sigma$(Be–**H**)	$\Delta\sigma$(**H**–X)
$LiH\cdots CH_4$	-0.09	-1.28		
$BeH_2\cdots CH_4$			-0.09	-0.18
$LiH\cdots C_2H_2$	0.24	-3.00		
$BeH_2\cdots C_2H_2$			0.18	-0.49
$BeH_2\cdots HCN$			0.44	-0.77
$BeH_2\cdots NH_4^+$			0.72	-4.08

The calculations were performed at MP2/aug-cc-pCVTZ

(aug-cc-pVTZsu1 for Li and Be atoms) level

The NMR shielding constants

- The shifts in the isotropic shielding constants of the proton acceptor hydrogen in LiH and BeH_2 are small.
- In weak van der Waals complexes they are negative (deshielding); in stronger bonded dimers they are positive (shielding).
- The protons in proton donors are deshielded. The largest shifts appears for the strongest complex, $BeH_2 \cdots NH_4^+$. The complexation shifts of the proton shielding constants of the proton donors exhibit an inverse correlation with the intermolecular distance.

The NMR shielding constants

- The shifts in the isotropic shielding constants of the proton acceptor hydrogen in LiH and BeH$_2$ are small.
- In weak van der Waals complexes they are negative (deshielding); in stronger bonded dimers they are positive (shielding).
- The protons in proton donors are deshielded. The largest shifts appears for the strongest complex, BeH$_2\cdots$NH$_4^+$. The complexation shifts of the proton shielding constants of the proton donors exhibit an inverse correlation with the intermolecular distance.

The NMR shielding constants

- The shifts in the isotropic shielding constants of the proton acceptor hydrogen in LiH and BeH_2 are small.
- In weak van der Waals complexes they are negative (deshielding); in stronger bonded dimers they are positive (shielding).
- The protons in proton donors are deshielded. The largest shifts appears for the strongest complex, $BeH_2 \cdots NH_4^+$. The complexation shifts of the proton shielding constants of the proton donors exhibit an inverse correlation with the intermolecular distance.

The indirect spin–spin coupling constants

	CCSD/aTsu1					**B3LYP/aTsu1**				
(Hz)	FC	DSO	PSO	SD	Sum	FC	DSO	PSO	SD	Sum
$LiH{\cdot}CH_4$										
$^{1h}J_{HH}$	-0.62	1.55	-1.33	...	**-0.40**	-0.61	1.55	-1.34	0.00	**-0.41**
$^{2h}J_{LiH}$	-0.09	0.17	-0.05	...	**0.03**	-0.05	0.17	-0.12	0.01	**0.02**
$^{2h}J_{HX}$	2.94	0.02	-0.04	...	**2.92**	4.57	0.02	-0.04	0.07	**4.62**
$^{3h}J_{LiX}$	0.98	-0.01	0.00	...	**0.98**	1.63	-0.01	0.01	0.01	**1.65**
$LiH{\cdot}C_2H_2$										
$^{1h}J_{HH}$	-1.06	2.32	-2.01	-0.06	**-0.81**	0.05	2.31	-2.04	-0.06	**0.26**
$^{2h}J_{LiH}$	-1.24	0.22	-0.06	0.03	**-1.06**	-1.59	0.22	-0.13	0.02	**-1.48**
$^{2h}J_{HX}$	9.43	0.11	-0.14	0.11	**9.51**	11.64	0.11	-0.15	0.13	**11.72**
$^{3h}J_{LiX}$	5.73	0.01	0.00	0.02	**5.76**	8.68	0.01	0.00	0.02	**8.70**

The comparison between different methods of calculations: the calculations were performed with the aug-cc-pVTZsu1 basis set

The indirect spin–spin coupling constants

Methodological aspects:

- CCSD and DFT(B3LYP) results agree reasonably. DFT reproduces well the signs and the order of magnitude calculated spin–spin couplings.
- The only disagreement appears for ${}^{1h}\mathrm{J}_{\mathrm{HH}}$ in $\mathrm{LiH}\cdots\mathrm{C}_2\mathrm{H}_2$ complex. However, this coupling constant is small.
- DFT may serve as an useful computational tool in case the CCSD method is too expensive.

The indirect spin–spin coupling constants

DFT/B3LYP	${}^{1h}\mathrm{J}_{HH}(Hz)$	${}^{1h}\mathrm{K}_{HH}\cdot 10^{-19}$	${}^{2h}\mathrm{J}_{BeH}$(Hz)	${}^{2h}\mathrm{K}_{BeH}\cdot 10^{-19}$
$BeH_2\cdots CH_4$	0.11	0.01	-0.11	0.07
$BeH_2\cdots C_2H_2$	-0.11	-0.01	0.16	-0.10
$BeH_2\cdots HCN$	-0.03	0.00	0.36	-0.22
$BeH_2\cdots NH_4^+$	6.09	0.51	0.79	-0.47

	${}^{2h}\mathrm{J}_{HX}$	${}^{2h}\mathrm{K}_{HX}\cdot 10^{-19}$	${}^{3h}\mathrm{J}_{BeX}$	${}^{3h}\mathrm{K}_{BeX}\cdot 10^{-19}$
$BeH_2\cdots CH_4$	0.95	0.31	-0.28	0.65
$BeH_2\cdots C_2H_2$	3.26	1.08	-1.42	3.35
$BeH_2\cdots HCN$	4.92	1.63	-1.94	4.57
$BeH_2\cdots NH_4^+$	-10.08	8.28	2.09	12.19

The calculations were performed at B3LYP/aug-cc-pVTZsu1 level

The indirect spin–spin coupling constants

- The short-range intermolecular proton-proton coupling^{1h}K$_{HH}$ are usually small. The largest one appears for the strongest complex, BeH$_2\cdots$NH$_4^+$. The values of J correlate with the interaction energy and the H$\cdots$H distance.
- The ^{2h}K$_{HX}$ between the hydrogen atom of BeH$_2$ and the carbon or nitrogen atoms of the proton donors are positive and much larger than the ^{1h}K$_{HH}$. They are mainly dominated by Fermi–contact term.
- The ^{3h}J$_{BeX}$ couplings despite the long Be-X separation are noticeable. The largest value is 2.09 Hz for BeH$_2\cdots$NH$_4^+$. The values correlate with the intermolecular distance.

The indirect spin–spin coupling constants

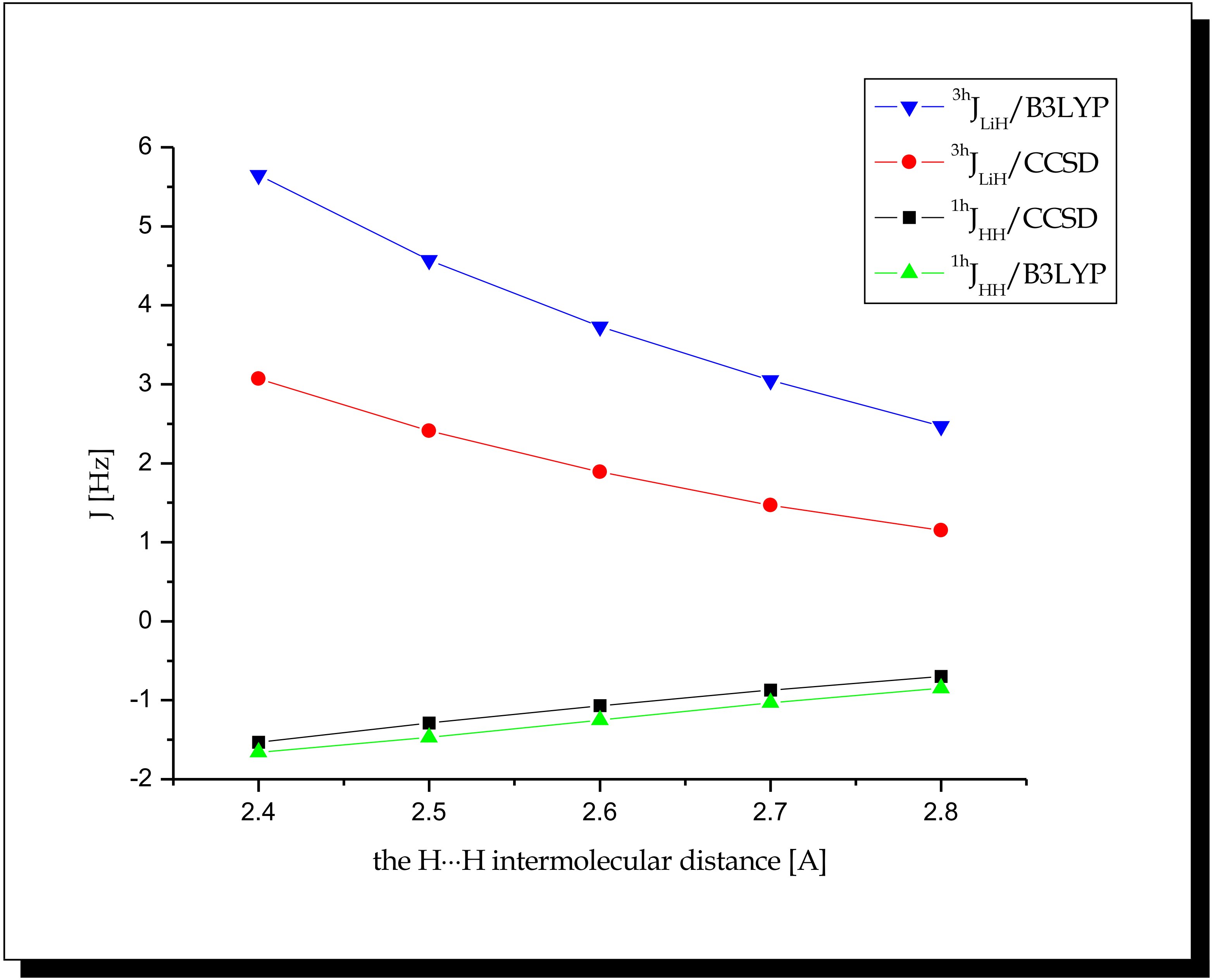

The indirect spin–spin coupling constants

Can a single curve be constructed from SSCC computed at equilibrium distance for a group of complexes with DHB and can that curve be useful for predicting intermolecular distances from experimentally measured coupling constants?

The answer is yes: two figures below show:

1. the dependence of the reduced intermolecular spin-spin coupling constants ${}^{2h}\mathrm{K}_{XH}$ on the dissociation energies D_e for six complexes studied.
2. the dependence of the reduced intermolecular spin-spin coupling constants ${}^{3h}\mathrm{K}_{BeX}$ of the $\mathrm{H}\cdots\mathrm{H}$ intermolecular distance.

The indirect ${}^{2h}\mathrm{K}_{XH}$ spin–spin coupling constants

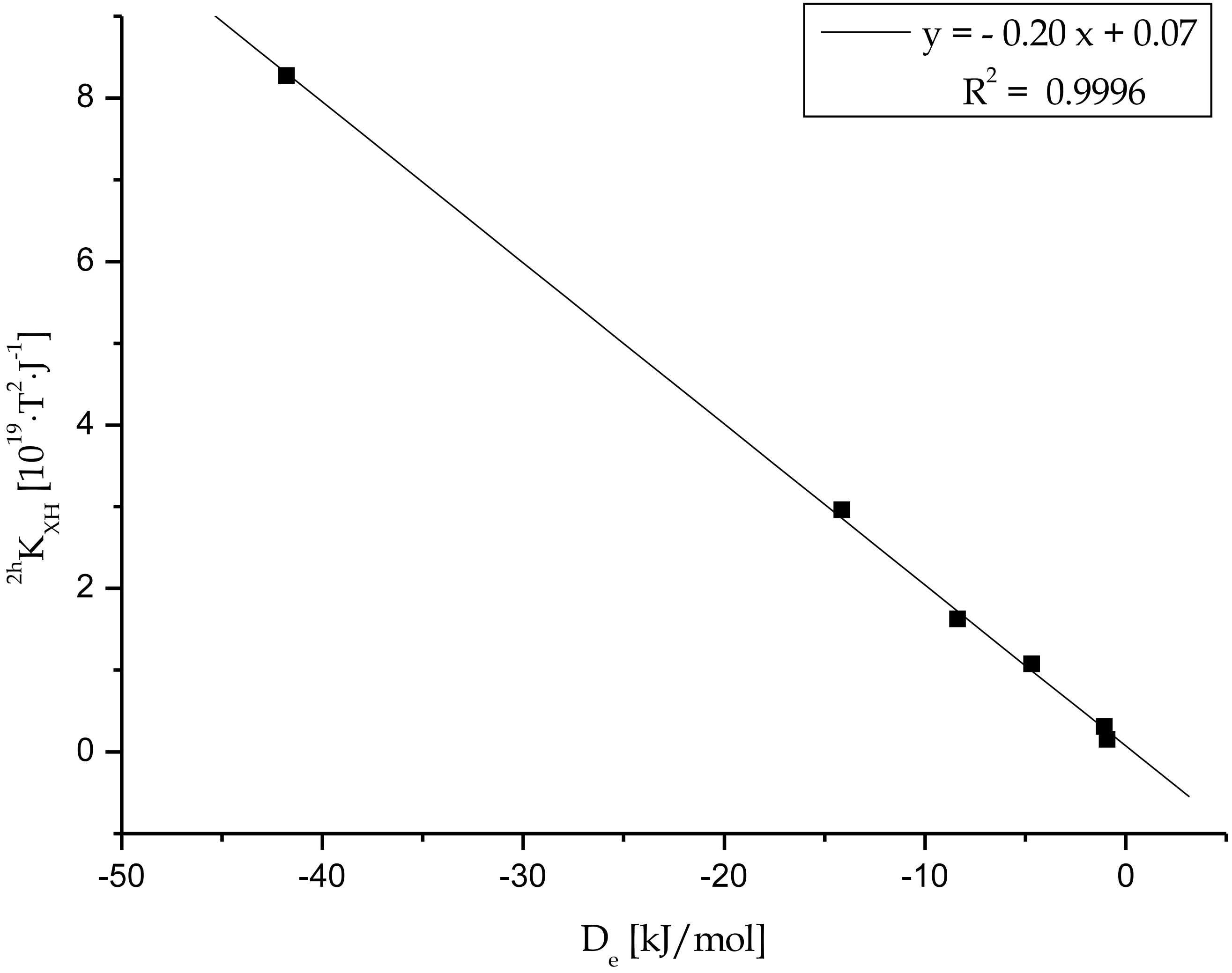

Figure 3

The indirect $^{3h}\mathbf{K}_{BeX}$ spin–spin coupling constants

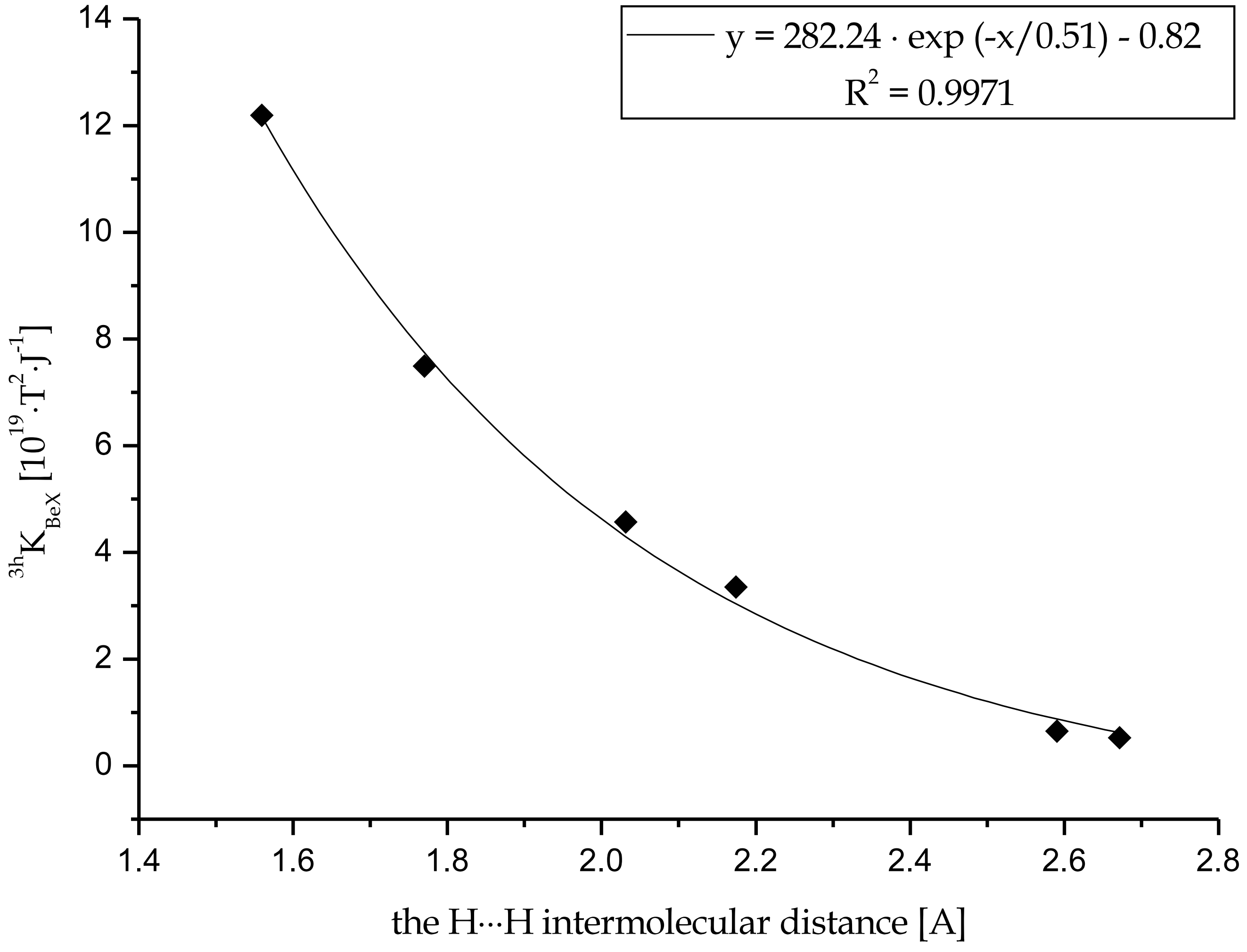

Figure 4

The distance dependence of the spin–spin coupling constants

Because DFT may serve as a useful tool for DHB-transmitted CC, we decided to use DFT to calculate the distance dependence of the intermolecular couplings, the calculation of which would otherwise be too expensive.

Methodological comparisons:

- The DFT and CCSD curves are similar but vertically displaced.
- The DFT constants are larger than the CCSD in absolute value

The indirect spin–spin coupling constants

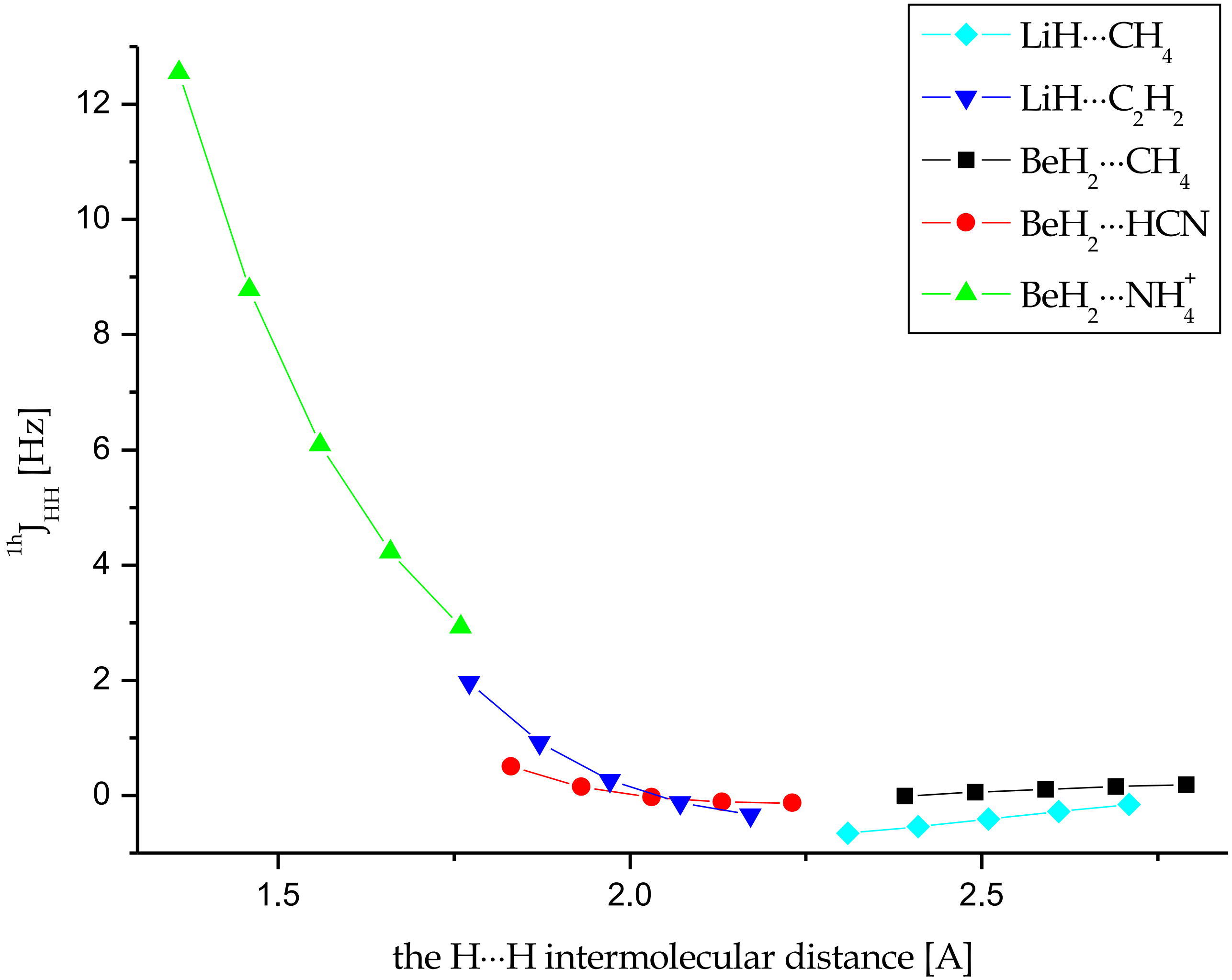

The indirect spin–spin coupling constants

- The distance dependence of the ${}^{1h}\mathrm{J}_{HH}$ intermolecular spin–spin coupling constants exhibits a consistent pattern for all complexes under study. It has a substantial values in two strongest complexes and decays steeply to zero. For $\mathrm{LiH}\cdots\mathrm{C_2H_2}$ it reaches zero and next it changes the sign.
- In weakly bonded complexes ${}^{1h}\mathrm{J}_{HH}$ is small and oscillates around zero and slowly decays to zero nearly linear with the intermolecular distance.
- At very large distances the value of ${}^{1h}\mathrm{J}_{HH}$ shows a little dependence on the nature of the donor, since in all cases it decays asymptotically to zero.

Conclusions

Based on the calculated intermolecular distances, interaction energies and decomposition of interaction energy, the complexes:

- can be divided into three groups:
  - weak van der Waals complexes,
  - dihydrogen–bonded complexes, comparable with the conventional H–bonds,
  - very strong complex of $BeH_2 \cdots NH_4^+$, which can be classified as very strong hydrogen bond.
- if the donors are listed in order to increasing proton-donating ability to LiH and BeH_2 (H_2<CH_4<HCCH<HCN<HNC<NH_4), then the $H \cdots H$ distance decreases from 2.7 to 1.6 Å.

Conclusions

- the decomposition of the ΔE_{int} is different for each group: for weaker van der Waals complexes - there is the large repulsive exchange term that outweighs the attractive electrostatic term and main binding is from the dispersion term; complexes, which the binding energy is comparable with the conventional H-bond are bound mainly by strong electrostatic and dispersion terms; the domination of the induction and the exchange terms are the main feature of the strong H-bond with the partly covalent character.
- the ${}^{2h}\mathrm{J}_{XH}$ coupling may serve as an indicator of the hydrogen bond type, since they have substantial values, which correlate with the interaction energy.

Conclusions

- SSCC transmitted through H-bond can be used to determined equilibrium intermolecular distances and relative binding energies for complexes, (^{3h}J$_{BeX}$ coupling can be fitted by the parabolic curve for the equilibrium structures of six complexes).

Acknowledgments

I wish to express my sincere appreciation to Professor P. Klein and Professor E. Arunan for inviting me for this meeting.

I am acknowledge with gratitude dr Magda Pecul-Kudelska and Hubert Cybulski for cooperation.

This work was also supported by Understanding Nano–Materials From the Quantum Perspective (NANOQUANT) Project, Contract Number MRTN-CT-2003-506842.

Coupling mechanisms

The calculations of ^{1}J(^{3}He,^{3}He) in He_2: the main FC coupling pathway is the overlap between the electronic clouds of both helium atoms and its efficiency does not depend on whether this corresponds to an attractive or repulsive interaction.
It has been known that the 'closed shell' interaction, which corresponds to spin exchange interactions (Fermi's correlation effects) defines a very efficient FC coupling pathway. The main transmission mechanism of the FC and the SD terms is the Fermi correlation interaction. The main feature of the transmission mechanism of the PSO term is the conservation of the electronic angular momentum.

In agreement with the work, these results indicate that if a spin-spin coupling is observed between two atoms belonging to proximate moieties, such coupling can not be used as a probe to determine the existence of either a weak bond or a covalent hydrogen-bond between them. In short, the FC term can be transmitted between two moieties as long as there is an overlap of their electronic clouds, it is irrelevant whether such an interaction is repulsive or attractive.